

Available online at www.sciencedirect.com

jmr&t
Journal of Materials Research and Technology
www.jmrt.com.br



Original Article

Spectroscopic studies of ZnO borate–tellurite glass doped with Eu_2O_3

Ali A. Ali^{a,*}, Hany M. Shaaban^b, Amany Abdallah^c^a Glass Research Department, National Research Centre, Dokki, 12622 Cairo, Egypt^b Chemistry Department, Faculty of Science, Tanta University, Tanta, Egypt^c Physics Department, Faculty of Science, Ain Shams University, Abbassia, 11556 Cairo, Egypt

ARTICLE INFO

Article history:

Received 24 February 2017

Accepted 27 June 2017

Available online xxx

Keywords:

Tellurite glasses

Europium glasses

Refractive index and nonlinear

optical devices

ABSTRACT

Optical, physical and thermal properties of glasses with composition $24\text{B}_2\text{O}_3 - (25 - x)\text{ZnO} - 51\text{TeO}_2, x\text{Eu}_2\text{O}_3$, mol% (where $x = 0.0, 0.5, 1$ and 3%) were studied. The density, crystallization temperature, oxygen packing density and glassy temperature were found to increase with the addition of Eu_2O_3 . The molar volume, optical band gap (E_g) and refractive index values were found to decrease with increasing Eu_2O_3 content. The FTIR measurements indicated that the continuous increase of europium concentration helped conversion of $[\text{BO}_3]$ to $[\text{BO}_4]$ groups in the base glass $\text{ZnO TeO}_2\text{-B}_2\text{O}_3$. Thermal analysis reveals that the glass transition temperature T_g , the glass thermal stability ΔT and the glass forming ability K_g increased by the addition of Eu_2O_3 . The transmission and absorption spectra of all glasses indicated that there is a decrease in the optical band gap E_g values due to the enhancement of the number of non-bridging oxygen (NBO) atoms with the addition of Eu_2O_3 . The studied glasses have high values of nonlinear refractive index n_2 and nonlinear optical susceptibility $\chi^{(3)}$ with a good thermal stability. Thus, such glasses have promised applications in nonlinear optical devices.

© 2017 Brazilian Metallurgical, Materials and Mining Association. Published by Elsevier Editora Ltda. This is an open access article under the CC BY-NC-ND license (<http://creativecommons.org/licenses/by-nc-nd/4.0/>).

1. Introduction

Glasses with tellurite offer distinct properties when compared with other glasses, such as good chemical durability and chemical resistance, high linear and non-linear refractive index, high transmittance especially in near infrared (NIR) to middle infrared (MIR) regions and high electrical conductivity [1,2]. They also are suitable candidates for use in fiber

optics, optical amplifiers, and laser, in addition to being widely used as photonic crystal fibers (PCFs); therefore, these glasses are considered as potential nonlinear materials [3–5]. Extensive studies were performed on B_2O_3 glasses for the past few decades because of their promised properties, which can be summarized as follows: 1 – glasses with low melting point, which can help save energy, 2 – high transparency, which is useful in optics, 3 – glasses with high thermal stability, 4 – easy to prepare and can dissolve a high concentration of rare

* Corresponding author.

E-mail: ali_nrc@hotmail.com (A.A. Ali).<http://dx.doi.org/10.1016/j.jmrt.2017.06.008>2238-7854/© 2017 Brazilian Metallurgical, Materials and Mining Association. Published by Elsevier Editora Ltda. This is an open access article under the CC BY-NC-ND license (<http://creativecommons.org/licenses/by-nc-nd/4.0/>).

earth ions, which means that these glasses are more suitable for optical device fabrication [6,7]. Formation of glass with two glass formers was known previously and is of scientific interest. The addition of TeO₂ into the borate network, which means the formation of glass with two glass formers, improves the transparency of the glass and its refractive index. Boro-tellurite glasses containing ZnO have a wide glass forming possibility and low ability to crystallize [8–10]. Doped glasses with rare earth ions have superior technological applications such as in fiber amplifiers, planar waveguides and display monitors of wavelength-converting devices [11–14]. It is known that europium is an element with optical active properties. The optical properties of trivalent europium ion are very sensitive to the surrounded atoms inside the glass, i.e. these properties are dependent on the glass composition. The selection of Eu³⁺ ions to add to the glass matrix is useful for the study of disordered materials, because europium has an energy level with simple structure and non-degenerate ground ⁷F₀ and emitting ⁵D₀ states [15,16]. We think that there is insufficient information regarding the presence of Eu³⁺ in the glasses of borate-tellurite composition. Therefore, it is very interesting to discover the relation between the change in the glass structural units and the linear and nonlinear properties of Eu³⁺ ions in borate-tellurite glasses.

2. Experimental

2.1. Glass preparation

In the present study, glasses having the composition 24B₂O₃ – (25 – x) ZnO – 51TeO₂, x Eu₂O₃, mol% (where x = 0.0, 0.5, 1 and 3%) were prepared using pure reagent grade H₃BO₃, ZnO, TeO₂ and Eu₂O₃ as starting materials. For each composition, the raw materials in the powder form were weighted accurately; then, they were mixed together using agate mortar and were melted in alumina crucibles at about 800 °C for 30 min in air. The glass melts were stirred occasionally with an alumina rod to achieve good homogeneity. The highly viscous melt was cast into a cylindrically shaped split mold of mild steel, and the produced glass was annealed at 450 °C in another furnace for 1 h, after which the furnace was switched off and the glass was allowed to cool gradually in situ for 24 h.

2.2. Density

The densities of these glasses (ρ) were determined by using Automatic Gas Pycnometers for True Density, Ultrapyc 1200e, and apparatus with helium gas.

2.3. FTIR

FTIR spectra of the glass samples were recorded at room temperature in the range of 400–4000 cm⁻¹ using Shimadzu FTIR 8400S spectrophotometer [resolution of 0.85 cm⁻¹ by KBr pellet technique]. The powdered samples were thoroughly mixed with dry KBr in the ratio of 1:20 by weight, and then the pellets were formed under a pressure of 9–10 tons.

2.4. DTA measurement

The thermal behaviors (differential thermal analysis DTA) of the finely powdered quenched samples were examined using SEATRAM Instrumentation Regulation, Labsys TM TG-DSC16 (Setaram, Caluire, France) under inert gas. The powder was heated in Pt-holder with another Pt-holder containing Al₂O₃ as a reference material. The results obtained were used as a guide for determining the required heat-treatment temperatures needed to induce crystallization in the samples, as will be shown later.

2.5. Optical absorption

The absorption and transmission spectra of the polished samples of 2-mm thickness at room temperature were measured in the range of 200–1800 nm using a recording spectrophotometer (JSCO Corp., V-570, Rev. 1.00).

3. Results and discussion

3.1. Density and molar volume

Although the measurements of the density (ρ) and the molar volume (V_m) are so simple tools, they are enough to tell us about the structural changes that occur in the studied glasses. Both of them depend on softening or compactness of structure of the studied sample. The molar volume V_m can give us a good idea about spatial distribution of the oxygen in the glass sample. It is known that the molar volume is a very perfect parameter to determine the compaction or expansion occurring in the glass structure. Molar volume is a bit better in the investigation of the structure and structural information than density. Therefore, we calculate the molar volume, V_m , for all studied glasses as follows:

$$V_m = \frac{\sum X_i M_i}{\rho} \quad (1)$$

where X_i is molar fraction of oxides used in the glass, M_i is molecular weight of oxides used and ρ is the density. As shown in Table 1, there is a decrease in the values of calculated molar volume with increase the amount of Eu ions added. The observed increase in ρ of the glass with increase in the contents of Eu₂O₃ may be attributed to the change in the coordination of boron atom in the glass sample. Replacing ZnO of less molar mass [ZnO = 81.39 amu] by Eu₂O₃ of larger molar mass content [Eu₂O₃ = 351.93 amu] leads to formation a large number of oxygen ions, which are available in glass structure. An observed decrease in the molar volume may be explained by the decrease in the bond length or the decrease in inter-atomic spacing among the atoms of glass network, which leads to a compact structure of the glass. The average distance between two boron atoms $\{d_{B-B}\}$ is calculated to estimate the change in the glass structure by addition of Eu₂O₃. The volume containing one mole of boron can be calculated with the given formula (V_m^z):

$$V_m^z = \frac{V_m}{2(1 - X_z)} \quad (2)$$

Table 1 – The physical properties of 24B₂O₃ – (25 – x) ZnO – 51TeO₂, x Eu₂O₃ glasses.

Glass sample	D (g cm ⁻³)	V _m (cm ³ /mol)	V _c (cm ³ /mol)	V _o (cm ³ /mol)	d _{B-B} (nm)	(OPD) (mol/l)
0	4.1	28.89	24.77	4.123	0.316	54.135
0.5	4.15	28.86	24.93	3.93	0.3158	54.676
1	4.2	28.84	25.103	3.737	0.3157	55.217
3	4.4	28.76	25.7	3.06	0.3155	56.075

where V_m is molar volume and X_z is the mole fraction of B₂O₃

$$\langle d_{z-z} \rangle = \sqrt[3]{\frac{V_m^z}{N_A}} \quad (3)$$

where N_A is the Avogadro number.

Crystalline volume V_c for all studied glass samples is calculated using the relation

$$V_c = \sum X_i V_i \quad (4)$$

where V_i is the molar volume of crystalline form of each component [17] (i.e., V_i = 28.148, 28.300, 14.5 and 47.557 cm³/mol for TeO₂, B₂O₃, ZnO and Eu₂O₃ by taking crystalline density 5.67, 2.46, 5.05 and 7.40 g/cm³ for TeO₂, B₂O₃, ZnO and Eu₂O₃, respectively). The volume deviation V_o (=V_m – V_c) is listed in Table 1, and we can notice that from this table that the V_m of the glasses is usually much greater than the corresponding values of V_c, which indicate the presence of excess structural volume in these samples; this is characteristic of their glassy nature.

The oxygen packing density (OPD) values were calculated from the equation relation as follows:

$$(\text{OPD}) = 1000 \times C \left(\frac{\rho}{M_i} \right) \quad (5)$$

where ρ, M_i and C are density, molar mass and number of oxygen ions present in the formula unit. The values of OPD increase with the increase in Eu₂O₃ content [18].

3.2. Thermal analysis

Fig. 1 represents the DTA measurements of all studied glass samples, from which it is observed that the glass transition temperature T_g increases with the addition of Eu₂O₃. The increase in T_g may be attributed to the increase in compactness as revealed by the decrease in the molar volume V_m and the increase in oxygen packing density (OPD) (Table 2). The T_g value increases by increasing the bond strength; thus, increase in T_g may also be attributed to high bond strength of Eu–O bond compared to Zn–O bond [19,20]. The (T_c) is the crystallization temperature. The glass thermal stability ΔT (T_g – T_c) increases with the increase in Eu₂O₃ content. The studied glasses have high thermal stability values where ΔT > 100 °C. Thus, high values of T_g and ΔT suggest that the addition of Eu₂O₃ to Zinc-boro tellurite glass increases its ability for fiber drawing. The glass forming ability K_g (Hurby factor) was given by the relation:

$$K_g = \frac{T_c - T_g}{T_m - T_c} \quad (6)$$

The K_g value increased with the increase in Eu₂O₃ for sample 2 (Eu₂O₃ content = 0.5). However, with further addition of Eu₂O₃, there is a small decrease in the Hurby factor values. This means that there is a little effect on the nucleation and crystallization processes inside the glass, or the ability for glass formation is considerably constant [21].

3.3. FTIR measurements

Generally the presence of different structural groups in the different glass samples can be identified by using measured infrared spectra of these glasses. In our study, the infrared spectra of base glass (free of Eu ions) were characterized by presence of several peaks at 469, 630, 940, 1100, 1230, 1390 and two small peaks at 1610 and 1640 cm⁻¹ as revealed in Fig. 2. We can classify these peaks into 3 regions. The first region lying around 600–700 cm⁻¹ can be attributed to the presence of B–O–B bending vibration bond in borate network, second region from 800 to 1200 cm⁻¹ which may be attributed to presence of B–O stretching presence in BO₄ units, and the third region extended from 1200 to 1600 cm⁻¹ due to B–O stretching of BO₃ units. Besides, the band from 2400 to 3600 cm⁻¹ was due

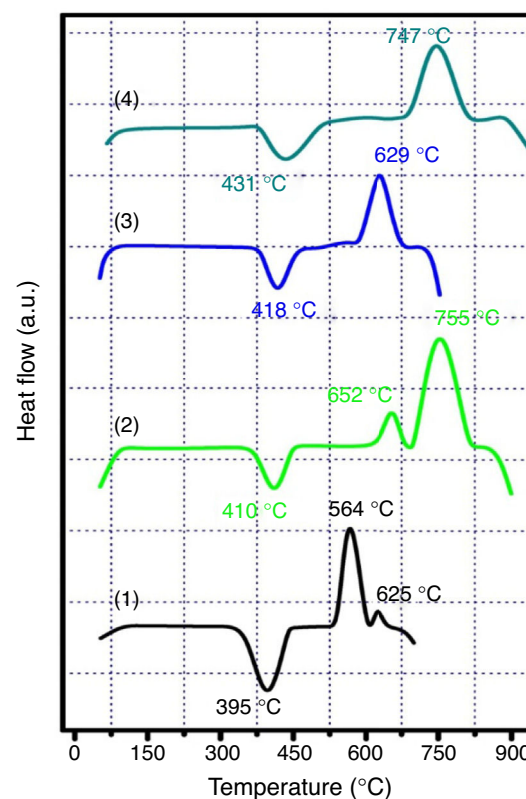


Fig. 1 – DTA of all studied samples. (1) Base, (2) 0.5 mol% Eu₂O₃, (3) 1 mol% Eu₂O₃, (4) 3 mol% Eu₂O₃.

Table 2 – The thermal properties of $24\text{B}_2\text{O}_3 - (25 - x)\text{ZnO} - 51\text{TeO}_2, x\text{Eu}_2\text{O}_3$ glasses.

Glass sample	T_g ($^{\circ}\text{C}$)	T_c ($^{\circ}\text{C}$)	T_m ($^{\circ}\text{C}$)	ΔT ($^{\circ}\text{C}$)	K_g
0.0	395	564	625	169	0.734
0.5	409	629	662	220	0.869
1	410	652	755	242	0.701
3	431	660	747	239	0.724

to O–H vibration of water group. There was a very weak band centered at 469 cm^{-1} , which may be attributed to the presence of the stretching vibration of equatorial and axial Te–O bonds in the TeO_4 trigonal bipyramids units, respectively [22–24].

Due to the absence of the band at about 806 cm^{-1} , we can say that the boroxol rings are absent in the network of our studied glass because it is well known that this band is assigned to the boroxol ring in borate glass network. Hence, the glass system contains $[\text{BO}_3]$ and $[\text{BO}_4]$ groups.

There are two broad bands, in all the samples, centered at 1360 cm^{-1} and 940 cm^{-1} , respectively, and are attributed to B–O bonds found in both $[\text{BO}_3]$ units and $[\text{BO}_4]$, respectively. The band at 1360 cm^{-1} is attributed to symmetric stretching vibration of B–O bond of orthoborate, pyroborate and metaborate groups in the form of $[\text{BO}_3]$ units [22,23] and the other band at 940 cm^{-1} is attributed to stretching vibration of B–O bond in $[\text{BO}_4]$ tetrahedral units of di-borate groups [22,24]. It was observed that the intensity of the first band decreased while the second increased progressively when europium oxide content increased by replacing an equal amount of ZnO from the glass system. Also, BO_3 band shifted toward lower wave number [1358–1352 cm^{-1}], whereas, BO_4 band shifted toward the longer wave number (961 cm^{-1}) with the rise in europium content. Hence, the continuous increase of europium concentration helped conversion of $[\text{BO}_3]$ to $[\text{BO}_4]$ groups in the base glass $\text{ZnO TeO}_2\text{-B}_2\text{O}_3$, which was already confirmed by the study of density and molar volumes.

3.4. Optical properties

The transmittance $T(\lambda)$ and the reflectance $R(\lambda)$ spectra in the wavelength range of 200–2500 nm for ZnO boro-tellurite glass

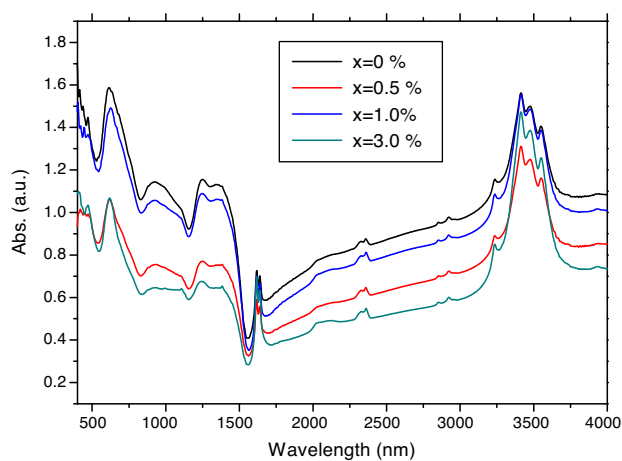


Fig. 2 – FTIR for base glass and glass doped with x mol% Eu_2O_3 .

doped with Eu_2O_3 are illustrated in Fig. 3. It is noticed that the studied samples are in the absorbing region where $R + T < 1$.

For each of the studied samples, the reflectance values show a gradual increase from 430 nm up to 450 nm followed by constant values up to 1800 nm. A sharp increase in transmittance values is observed at 430 nm followed by a gradual increase up to 830 nm; thereafter, it became constant. It is noticed that T values decrease with the increase in Eu content, and an absorption region between 500 and 830 nm was observed for Eu-containing glass. Such absorption was attributed to the optical transitions from ${}^7\text{F}_0$ to ${}^5\text{D}_4$, ${}^5\text{G}_4$, ${}^5\text{L}_6$, ${}^5\text{D}_3$, ${}^5\text{D}_2$, ${}^5\text{D}_1$ and ${}^5\text{D}_0$ of Eu^{3+} ions [25].

The absolute values of $T(\lambda)$ and $R(\lambda)$ are used to calculate the optical constants, the optical absorption coefficient (α), the absorption index (k) and the refractive index (n) using the following relations [26]:

$$\alpha = \frac{1}{t} \ln \left[\frac{(1-R)^2}{2T} + \sqrt{\frac{(1-R)^2}{4T^2} + R^2} \right] \quad (7)$$

$$k = \frac{\alpha\lambda}{4\pi} \quad (8)$$

$$n = \frac{1+R}{(1-R)} + \sqrt{\frac{4R}{(1-R)^2} - k^2} \quad (9)$$

Increase in (α) values was observed with the increase in Eu content as indicated in Fig. 4. The absorption peaks observed from 850 to 430 nm for Eu-containing samples are attributed to the presence of color centers induced by Eu ions.

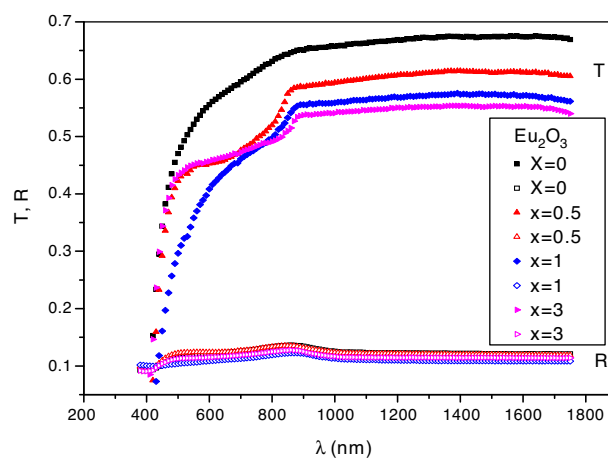


Fig. 3 – The transmittance $T(\lambda)$ and the reflectance $R(\lambda)$ spectra for ZnO boro-tellurite glasses doped with $x\text{Eu}_2\text{O}_3$.

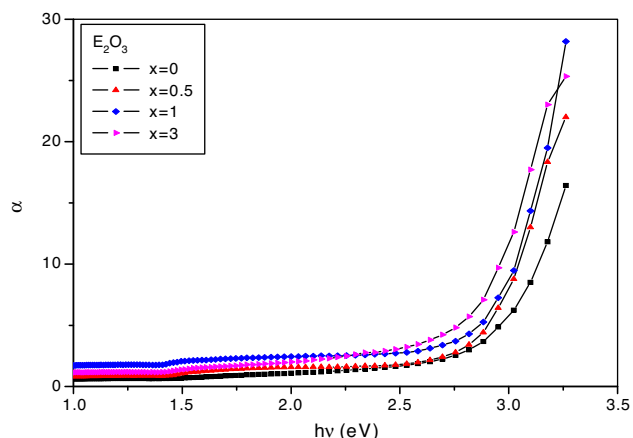


Fig. 4 – The absorption coefficient (α) at different photon energies as function of Eu_2O_3 .

The relationship between the optical absorption coefficient (α) and the photon energy was described by Tauc [27].

$$(\alpha h\nu) = B(h\nu - E_g)^r \quad (10)$$

where B is constant, $h\nu$ is the incident photon energy, E_g is the optical band gap of the glass sample, and r depends upon the type of transition. The value of r is $1/2$ for the allowed direct transition, whereas it is 2 for the indirect transition. The indirect band gap (E_g) was estimated by extrapolating the straight line part of the relation between $(\alpha h\nu)^{1/2}$ and photon energy at $(\alpha h\nu)^{1/2} = 0$, as shown in Fig. 5. It is clear that there is a decrease in the E_g values with the increase in Eu_2O_3 content as shown in Table 2. This behavior is attributed to the structural changes in the glass network with the addition of Eu_2O_3 . The addition of Eu_2O_3 enhances the number of non-bridging oxygen (NBO) atoms in the glass network. NBO's ions shift the edge of valence band toward the conduction band [28]. This leads to decreases in the optical band gap values.

The refractive index (n) values (determined from Eq. (9)) at different wavelengths are plotted in Fig. 6. It is noticed from

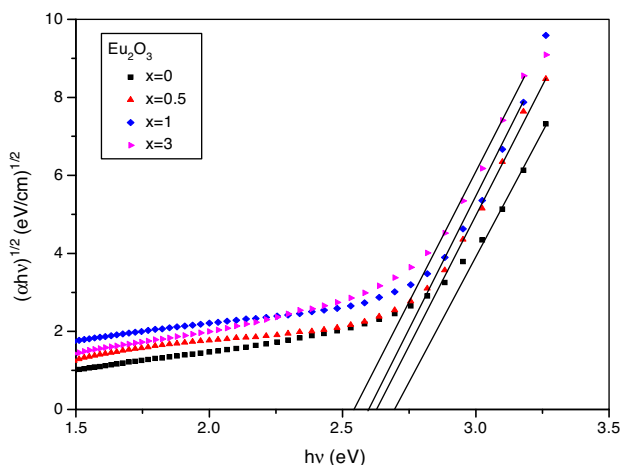


Fig. 5 – The relation between $(\alpha h\nu)^{1/2}$ and photon energy as function of Eu_2O_3 .

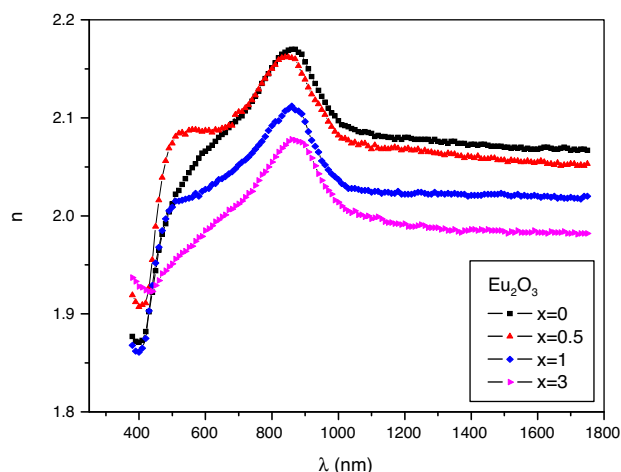


Fig. 6 – The relation between refractive index (n) and wavelength (λ) as function of Eu_2O_3 .

Fig. 6 that the refractive index values decrease with increasing Eu_2O_3 content. Fig. 6 represents a peak with n_{max} value at ≈ 840 nm, which shifts to longer wavelength with increasing Eu_2O_3 content. The values of n and n_{max} decreased with the addition of Eu_2O_3 . At $\lambda > 1100$ nm, a normal dispersion is observed. Such a dispersion is analyzed by Wemple and DiDomenico (WDD) single oscillator model [29,30]. The (WDD) model suggests that the relation between n and $h\nu$ is given in the following equation:

$$(n^2 - 1)^{-1} = \frac{E_o}{E_d} - \frac{1}{E_o E_d} (h\nu)^2 \quad (11)$$

where E_o is the effective oscillator energy and E_d is the dispersion energy, which measures the strength of the inter-band optical transitions. $(n^2 - 1)^{-1}$ is plotted versus $(h\nu)^2$ as shown in Fig. 7. E_o and E_d values are determined from the slope and intercept of the extrapolated straight line and listed in Table 3. The effective oscillator energy, E_o , is related to the bond energy of the chemical bonds existing in the glass matrix [31]. Thus, the formation of non-bridged oxygen ions decreases the

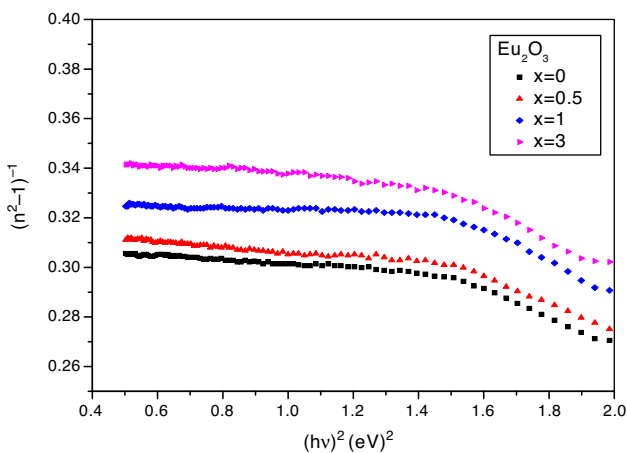


Fig. 7 – The relation between $(n^2 - 1)^{-1}$ and $(h\nu)^2$ as function of Eu_2O_3 .

Table 3 – The optical properties and nonlinear refractive index n_2 and nonlinear optical susceptibility $\chi^{(3)}$ for $24\text{B}_2\text{O}_3 - (25 - x) \text{ZnO} - 51\text{TeO}_2, x \text{Eu}_2\text{O}_3$ glasses.

X	E_g (eV)	E_o (eV)	E_d (eV)	ε_∞	β	ε_L	$\chi^{(3)}$ (esu)	n_2 (esu)
0	2.695	6.120	19.758	4.230	0.277	4.330	4.737×10^{-11}	8.694×10^{-10}
0.5	2.624	5.976	17.743	4.161	0.276	4.308	3.390×10^{-11}	6.421×10^{-10}
1	2.594	9.746	29.827	4.061	0.275	4.113	3.827×10^{-11}	7.156×10^{-10}
3	2.541	5.613	17.216	3.881	0.265	3.962	4.475×10^{-11}	8.243×10^{-10}

fraction of covalent and increases the fraction of ionic bonds, which have lower bond energy than the covalent bonds. This behavior could explain the decrease of E_o value with increase in Eu_2O_3 content.

The dielectric constant at infinite frequency ε_∞ is determined from extrapolation of the straight line with the ordinate axis at $(h\nu)^2=0$. Petkov et al. [32] proposed the relations between the dispersion energy E_d and other physical parameters as:

$$E_d = \beta N_c Z_a N_e \quad (12)$$

where N_c is the coordination number of the cation, which is the nearest neighbor to the anion, Z_a is the formula chemical valence of the anion, N_e is the effective number of valence electrons per anion and β is a parameter between 0.26 ± 0.04 eV for ionic materials and 0.37 ± 0.05 eV for covalent materials. Using the calculated β values of Eu_2O_3 -doped and -undoped Zn-boro-tellurite glass (Table 2) and the values of $N_c=4$, $Z_a=2$ and $N_e=8$ [26,29], the obtained β values are around 0.261. These results confirmed that Eu_2O_3 -doped glasses have more ionic character than the undoped glass, which could be attributed to the increase in the number of non-bridging oxygen (NBO) atoms in the glass network.

The refractive index, n , is related to the lattice dielectric constant (ε_L) by the following equation [33]:

$$n = \varepsilon_L - \left(\frac{e^2}{4\pi^2 \varepsilon_0 c^2} \right) \left(\frac{N}{m^*} \right) \lambda \quad (13)$$

where e is the electronic charge, ε_0 is the permittivity of free space, c is the speed of light and N/m^* is the ratio of the carrier concentration to the effective mass. Fig. 8 indicates a linear relation between n^2 and λ^2 , for Eu_2O_3 -doped and -undoped glasses, which is consistent with Eq. (13). The ε_L values are determined from the extrapolation of the linear relation to $\lambda^2=0$. It is noticed that $\varepsilon_\infty < \varepsilon_L$, which was attributed to free charge carrier contribution [34].

3.5. Nonlinear optical properties

Several theoretical models have been proposed for calculation of the third-order susceptibility $\chi^{(3)}$ and the non-linear index n_2 [35–37]. In this work, the model suggested by Tichy et al. [38] is applied. They combine the Miller's generalized rule [39] with the static refractive index, which is evaluated from the WDD single oscillator model [29]. According to their proposed model, $\chi^{(3)}$ and n_2 are given by the following relations:

$$\chi^{(3)} = \frac{A}{(4\pi)^4} \left(\frac{E_d}{E_o} \right)^4 = \frac{A}{(4\pi)^4} (n_o^2 - 1)^4$$

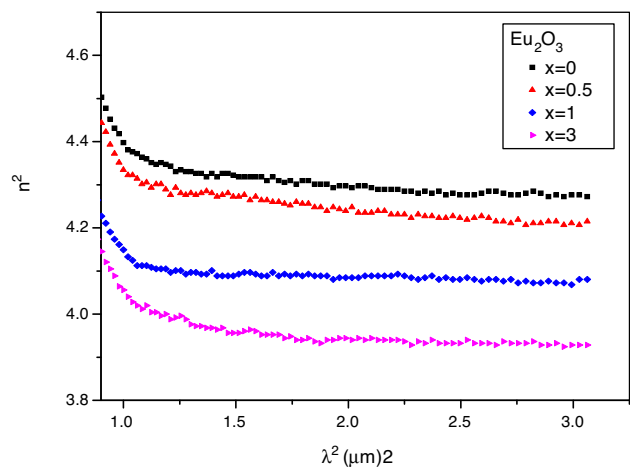


Fig. 8 – The relation between (n^2) and $(\lambda)^2$ as function of Eu_2O_3 .

$$n_2 = \frac{12\pi\chi^{(3)}}{n_o}$$

where $A = 1.7 \times 10^{-11}$ and n_o is the static refractive index. From Eq. (11), as $h\nu \rightarrow 0$, then $n = n_o$, i.e.,

$$n_o = \sqrt{1 + \frac{E_d}{E_o}}$$

The third-order susceptibility $\chi^{(3)}$ and the non-linear index n_2 values for the studied glasses are listed in Table 3. It is observed from Table 3 that $\chi^{(3)}$ and n_2 values decreased with the addition of 0.5 mol Eu_2O_3 . The observed decrease in Eu_2O_3 -doped glass could be attributed to the replacement of a higher polarizable ZnO by a lower polarizable Eu_2O_3 .

However, the $\chi^{(3)}$ values indicate a gradual increase with further increasing Eu_2O_3 concentration. This behavior could be explained by the enhancement of excitation electron with the increasing Eu_2O_3 concentration [40].

ZnO borate-tellurite glass doped with Eu_2O_3 showed higher values of nonlinear refractive index n_2 and nonlinear optical susceptibility $\chi^{(3)}$ than that reported for heavy elements, such as borate and silicate glasses [41,42]. These results suggested that Eu_2O_3 -doped and -undoped ZnO boro-tellurite glasses have promising applications in nonlinear optical switching devices [40,43].

4. Conclusion

Glasses of composition $24\text{B}_2\text{O}_3 - (25 - x) \text{ZnO} - 51\text{TeO}_2, x \text{Eu}_2\text{O}_3$, mol% (where $x=0.0, 0.5, 1$, and 3%) were prepared.

- Density of studied glasses was measured and found to decrease with increasing the Eu_2O_3 content, whereas the molar volume of the same studied glasses were found to decrease.
- Crystalline volume V_c for all studied glass samples were calculated, and the volume deviation V_o were estimated and found to decrease with increasing the Eu_2O_3 content.
- FTIR spectra were characterized by the presence of several peaks at 469, 630, 940, 1100, 1230, 1390 and two small peaks at 1610 and 1640 cm^{-1} .
- By addition of Eu_2O_3 , there was a change in intensity and position of the peaks related to change from $[\text{BO}_3]$ to $[\text{BO}_4]$ groups.
- The glass thermal stability $\Delta T (T_g - T_c)$ increases with the increase in Eu_2O_3 content.
- The glass forming ability K_g (Hurby factor) increased with the increase in Eu_2O_3 .
- The E_g values were with increasing in Eu_2O_3 content, which attributed to the Enhancement of the number of non-bridging oxygen (NBO) atoms in the glass network.
- The studied glasses have high values of nonlinear refractive index n_2 and nonlinear Optical susceptibility $\chi^{(3)}$.

The results obtained indicated that ZnO boro-tellurite glass doped with Eu_2O_3 has high nonlinear optical property values with good thermal stability, which make these glasses suitable candidates for their application in fiber optics and nonlinear devices and broadband optical amplifiers.

Conflicts of interest

The authors declare no conflicts of interest.

REFERENCES

- Hayakawa T, Hayakawa M, Nogami M, Thomas MP. Nonlinear optical properties and glass structure for $\text{MO-Nb}_2\text{O}_5\text{-TeO}_2$ ($\text{M} = \text{Zn, Mg, Ca, Sr, Ba}$) glasses. *Opt Mater* 2010;32:448–55.
- Stambouli W, Elhouichet H, Gelloz B, Ferid M, Koshida N. Energy transfer induced Eu^{3+} photoluminescence enhancement in tellurite glass. *J Lumin* 2012;132:205–9.
- Ravi Kanth Kumar VV, George AK, Knight JC, Russell Pst J. Tellurite photonic crystal fiber. *Opt Exp* 2003;11(20):2641–3245.
- Fares F, Jlassi I, Elhouichet H, Férid M. Investigations of thermal, structural and optical properties of tellurite glass with WO_3 adding. *J Non-Cryst Solids* 2014;396–397:1–7.
- El-Mallawany RA. *Tellurite glasses handbook – physical properties and data*. Boca Raton, FL: CRC Press; 2002.
- Mahraz ZAS, Sahar MR, Ghoshal SK, Reza Dousti M. Concentration dependent luminescence quenching of Er^{3+} doped zinc boro-tellurite glass. *J Lumin* 2013;144:139–45.
- Arul Rayappan I, Marimuthu K. Luminescence spectra and structure of Er^{3+} doped alkali borate and fluoroborate glasses. *J Phys Chem Solids* 2013;74:1570–7.
- Selvaraju K, Marimuthu K. Structural and spectroscopic studies on concentration dependent Er^{3+} doped boro-tellurite glasses. *J Lumin* 2012;132:1171–8.
- GayathriPavani P, Sadhana K, Chandra Mouli V. Optical, physical and structural studies of boro-zinc tellurite glasses. *Physica B* 2011;406:1242–7.
- Selvaraju K, Marimuthu K. Structural and spectroscopic studies on Er^{3+} doped boro-tellurite glasses. *Physica B* 2012;407:1086–93.
- Stambouli W, Elhouichet H, Barthou C, Férid M. Energy transfer induced photoluminescence improvement in $\text{Er}^{3+}/\text{Ce}^{3+}/\text{Yb}^{3+}$ tri-doped tellurite glass. *J Alloys Compd* 2013;580:310–5.
- Lu L, Nie Q, Xu T, Dai S, Shen X, Zhang X. Up-conversion luminescence of $\text{Er}^{3+}/\text{Yb}^{3+}/\text{Nd}^{3+}$ -codoped tellurite glasses. *J Lumin* 2007;126:677–81.
- Liao M, Hu L, Fang Y, Zhang J, Sun H, Xu S, et al. Upconversion properties of Er^{3+} , Yb^{3+} and Tm^{3+} codoped fluorophosphate glasses. *Spectrochim Acta A* 2007;68:531–5.
- Chimalawong P, Kaewkhao J, Kedkaew C, Limsuwan P. Optical and electronic polarizability investigation of Nd^{3+} -doped soda-lime silicate glasses. *J Phys Chem Solids* 2012;71:965–70.
- Stambouli W, Elhouichet H, Gelloz B, Ferid M. Optical and spectroscopic properties of Eu-doped tellurite glasses and glass ceramics. *J Lumin* 2013;138:201–8.
- Dimitrov V, Komatsu T. An interpretation of optical properties of oxides and oxide glasses in terms of the electronic polarizability and average single bond strength. *J Univ Chem Technol Metall* 2010;45:219–50.
- Dahiya S, Punia R, Murugavel S, Maan AS. Structural and other physical properties of lithium doped bismuth zinc vanadate semiconducting glassy system. *J Mol Struct* 2015;1079:189–93.
- Yung SW, Chiang HY, Lai YS, Wu FB, Fu C, Lee Y-M. Thermal, optical and structural properties of Tb doped zinc aluminum phosphate glasses. *Ceram Int* 2015;41:877–88.
- Abdel-Baki M, Abdel-Wahab FA, El-Diasty F. One-photon band gap engineering of borate glass doped with ZnO for photonics applications. *J Appl Phys* 2012;111(7):073506.
- Dult M, RS Kundu RS, Berwal N, Punia R, Kishore N. Manganese modified structural and optical properties of bismuth silicate glasses. *J Mol Struct* 2015;1089:32–7.
- Monteiro G, Santos LF, Pereira JCG, Almeida RM. Optical and spectroscopic properties of germane-tellurite glasses. *J Non-Cryst Solids* 1994;357:2695–701.
- Arifin R, Sahar Md R, Sulhadi. FTIR spectroscopy study on tellurite doped Eu_2O_3 glass. *Solid State Sci Technol* 2007;15:122–6.
- El-Fayoumi MAK, Farouk MJ. Structural properties of Li-borate glasses doped with Sm^{3+} and Eu^{3+} ions. *J Alloys Compd* 2009;482:356–60.
- Kaur M, Singh SP, Mudahar DS, Mudahar GS. Structural investigation of $\text{B}_2\text{O}_3\text{-Li}_2\text{CO}_3\text{-Al}_2\text{O}_3$ glasses by molar volume measurements and FTIR. *Mater Phys Mech* 2012;15:66–73.
- Sun XY, Jiang DG, Chen SW, Zheng GT, Huang SM, Gu M, et al. Eu^{3+} -activated borogermanate scintillating glass with a high Gd_2O_3 content. *J Am Ceram Soc* 2013;96:1483–9.
- Moss TS. *Optical properties in semiconductors*. London: Butterworths; 1959.
- Tauc J. *Amorphous and liquid semiconductors*. New York: Plenum Press; 1974.
- Saddeek BY, Shaaban RE, Moustafa E, Moustafa MH. Spectroscopic properties, electronic polarizability, and optical basicity of $\text{Bi}_2\text{O}_3\text{-Li}_2\text{O-B}_2\text{O}_3$ glasses. *Physica B* 2008;403:2399–407.
- Wemple SH, Didomenico M Jr. Behavior of the electronic dielectric constant in covalent and ionic materials. *Phys Rev B* 1971;3:1338–51.

- [30] Wemple SH. Refractive-index behavior of amorphous semiconductors and glasses. *Phys Rev B* 1973;7-8: 3767-77.
- [31] Pedrotti FL, Pedrotti LS. *Introduction to optics*. London: Prentice-Hall International, Inc; 1993.
- [32] Petkov K, Tichyp L, Kincl N, Todorov R. Effect of thallium on the optical properties and structure of thin As-S-Tl films. *J Optoelectron Adv Mater* 2005;7(5):2587-94.
- [33] Edward DP. *Handbook of optical constants of solids*. New York: Academic Press Handbook; 1985.
- [34] El-Nahass MM, Dongol M, Abou-Zaied M, El-Denglawey M. The compositional dependence of the structural and optical properties of amorphous As₂₀Se_{80-x}Tl_x films. *Physica B* 2005;386:179-87.
- [35] Sheik-Bahae M, Hagan DJ, Stryland EW. Dispersion and band-gap scaling of the electronic Kerr effect in solids associated with two-photon absorption. *Phys Rev Lett* 1990;65:96.
- [36] Hajto E, Ewen PJS, Owen AE. Linear and nonlinear optical properties of chalcogenide glasses. *J Non-Cryst Solids* 1993;164-166:901-4.
- [37] Petkov K, Ewen PJS. Photo induced changes in the linear and non-linear optical properties of chalcogenide glasses. *J Non-Cryst Solids* 1999;249:150-9.
- [38] Tichý L, Tichá H, Handlř K. Some thermally and optically induced changes of optical properties of amorphous As₃₈S₆₂ films. *J Mater Sci* 1988;23:229-34.
- [39] Wyne JJ. Optical third-order mixing in GaAs, Ge, Si, and InAs. *Phys Rev* 1969;178:1295.
- [40] Azlan MN, Halimah MK, Sidek HAA. Linear and nonlinear optical properties of erbium doped zinc borotellurite glass system. *J Lumin* 2017;181:400-6.
- [41] Bala R, Agarwal A, Sanghi S, Singh N. Effect of Bi₂O₃ on nonlinear optical properties of ZnO-Bi₂O₃-SiO₂ glasses. *Opt Mater* 2013;36:352-6.
- [42] Kondo Y, Ono M, Kageyama K, Reys K, Sugimoto N. Gain characteristics of 6 cm-long Er-doped bismuthate waveguide. *Electron Lett* 2005;41(6):317-8.
- [43] Wanga YH, Wang YM, Lu JD, Ji LL, Zang RG, Wang RW. Nonlinear optical properties of Cu nanoclusters by ion implantation in silicate glass. *Opt Commun* 2010;283(3):486-9.